Journal of the European Ceramic Society 19 (1999) 2359–2366

PII: S0955-2219(99)00106-5
0955-2219/99/$ - see front matter

Potential of the Sinter-HIP-technique for the Development of High-temperature Resistant Si_3N_4-ceramics

M. J. Hoffmann,* A. Geyer[1] and R. Oberacker

University of Karlsruhe, Institute for Ceramics in Mechanical Engineering, Haid-und-Neu-Str. 7, D-76131 Karlsruhe, Germany

Abstract

Silicon nitride ceramics were densified with the sintering additives Y_2O_3 and SiO_2 by a two-step sinter-HIP-process. Three compositions with additive contents between 2 and 7 wt% Y_2O_3 were prepared to study the influence of the processing conditions on the mechanical properties. The minimum additive content required for nearly complete densification (>98.5%) was only 2 wt% Y_2O_3. However, densification was limited to certain Y_2O_3/SiO_2 ratios. The additive-rich samples revealed a mean strength at room temperature up to 800 MPa which degrades at 1400°C. The material with only 2 wt% Y_2O_3 has a room temperature strength of ~500 MPa, but no strength degradation up to 1400°C. The lower strength correlates with a pronounced increase in brittleness with a decreasing additive content indicated by a fracture toughness of only 2·5 $MPam^{1/2}$ for composition 2/0. The investigated materials exhibit a relatively high creep resistance at 1400°C with creep rates down to $1{\cdot}5\times10^{-9}$ s^{-1}. © *1999 Elsevier Science Ltd. All rights reserved.*

Keywords: hot isostatic pressing, creep, mechanical properties, strength, toughness, Si_3N_4.

1 Introduction

Silicon nitride ceramics have been intensively studied over the last three decades because of their exceptional mechanical properties at room as well as higher temperatures. The material behaviour is apparently attributed to the highly covalent Si–N bond giving a high strength to the grains, but also a low diffusivity of Si and N even at very high temperatures. Since good mechanical properties of monolithic Si_3N_4 ceramics can only be obtained in fully dense materials, sintering additives must be added to silicon nitride ceramics. The additives form an amorphous or partially crystalline secondary phase after sintering and have a strong impact on properties. Another main feature of silicon nitride ceramics is the anisotropic grain growth in the presence of a liquid phase formed by the additives and the silica impurity of the silicon nitride powder. The growth anisotropy of Si_3N_4 leads to a self-reinforced microstructure due to the formation of needle-like grains during densification.[1,2] However, the self-reinforcement requires not only elongated grains, but also a weak interface between the silicon nitride grains in order to activate toughening mechanisms such as crack bridging, pull-out, debonding or crack deflection.[3]

The secondary phase, necessary for high strength and toughness at room temperature, limits on the other hand the high-temperature resistance because of its viscosity decrease above the glass transition temperature. For this reason it is easy to understand that high temperature resistant Si_3N_4 ceramics demand a highly refractive grain boundary phase after complete densification. In the past, several strategies have been explored to optimise the high temperature properties: (i) the devitrification of the amorphous grain boundary phase by a post sintering heat treatment;[4] (ii) the formation of a transient liquid phase, which could be dissolved in the Si_3N_4 crystal lattice during densification (formation of a solid solution)[5,6] and (iii) the reduction of the overall additive content in combination with the use of refractive additives, such as Y_2O_3 or rare earth oxides. The last method is combined with high manufacturing costs since densification requires hot-pressing or hot isostatic pressing (HIP).

The current work was initiated to analyse the potential of a sinter-HIP-process as an alternative densification method to hot-pressing or glass-

*To whom correspondence should be addressed. Fax: +49-721-6088891; e-mail: michael.hoffmann@mach.uni-karlsruhe.de
[1]Now with: HWP Stuttgart, Germany.

encapsulated HIPing. The technique is comparable to gas pressure sintering, but the final pressure is about one order of magnitude higher. All experiments were performed in the additive system Y_2O_3-SiO_2 because of the well-known phase relationships with Si_3N_4[7] and the good high-temperature stability of the pseudo-binary compounds.

2 Experimental Procedure

Mixtures of the silicon nitride powder (E 10 grade, Ube Industries Ltd, Japan) and different amounts and ratios of the sintering additives Y_2O_3 (grade fine, H.C. Starck, Germany) and SiO_2 (Ox-50, Degussa, Germany) were milled in a planetary mill with sialon balls for 8 h in ethanol, dried in a rotary evaporator and sieved. The investigated specimen compositions are listed in Table 1. Consolidation of the powders to rectangular plates of the dimension ($65\times45\times10$ mm^3) was obtained by uniaxial pressing in a steel die at a pressure of 17 MPa and subsequent isostatic pressing at 600 MPa. Pressure-assisted sintering experiments were performed in a hot-isostatic press [QIH-6, ASEA, Columbus (Ohio), USA] in a temperature range between 1900 and 1950°C and isostatic pressures between 10 and 100 MPa. The temperature was controlled by W/Rh-thermocouple.

All specimens were densified by a two-step sinter-HIP-process without glass-encapsulation in a pyrolytic BN-crucible without powder bed. The measured weight loss was $<1\%$. Dynamic dilatometry was applied during sintering for the analysis of the densification behaviour and for optimisation of the sintering conditions. Details of the used HIP-dilatometer are described in Ref. 8. Samples used for the dilatometric studies had a dimension of $8\times8\times24$ mm^3 and were prepared from larger rectangular green compacts by dry cutting. The densities of the sintered samples were determined by Archimedes' method as well as the water intrusion method. In order to characterise the microstructure, specimens were ground and polished through 1 μm diamond abrasive. Residual microporosity was observed by optical microscopy whereas size and morphology of the silicon nitride grains were characterised by scanning electron microscopy (SEM) of plasma etched[9] and gold-coated surfaces. The α/β-Si_3N_4-ratio and crystalline secondary phases were determined by X-ray diffraction analysis.

The strength between room temperature and 1475°C was determined by 4-point bending tests with an outer and inner span of 40/20 mm and a sample cross-section of 3×4 mm^2. Samples with a sharp notch, initiated by the bridge method,[10] were prepared to measure the fracture toughness in 4-point bending. The long-term behaviour of the different materials was characterised by 4-point bend creep tests of pre-oxidised samples between 1300 and 1450°C and loads between 100 and 200 MPa. The pre-oxidation for 200 h at 1400°C in air was performed in order to stabilise the microstructure with respect to the crystallisation of secondary phases.

3 Results and Discussion

3.1 Analysis of the densification behaviour

The sinterability of silicon nitride ceramics strongly depend on the viscosity and the volume fraction of the liquid phase. The composition of the liquid phase is determined by the additives of the starting composition and the impurities of the raw materials. The most important impurity is the oxygen content of the silicon nitride powder (1·5 wt% O for the current powder). For additive rich starting compositions (>10 wt%), the oxygen content does not have a significant influence on the densification behaviour, but with the reduction of the additives, the oxygen content of the silicon nitride powder has to be taken into account. Under the assumption that most of the oxygen is present on the silicon nitride particle surfaces in the form of silica, a Y_2O_3/SiO_2 volume ratio could be calculated. For typical HIP-compositions, containing only 2 wt% Y_2O_3 (2/0, Table 1), this ratio reaches nearly 1:1. Since silica rich melts are characterised by high viscosities, densification becomes more difficult.

A complete densification by a two-step sinter-HIP-process requires the achievement of closed porosity in the low pressure step. Because of the reduced sinterability with decreasing additive content pore closure becomes very sensitive to the sintering parameters temperature, pressure and time.

Table 1. Compositions and sintering conditions for the low-pressure stage

Sample	*Si_3N_4[a] [wt%]*	*Y_2O_3 [wt%]*	*SiO_2[wt%]*	*Sintering temperature [°C]*	*Sintering time [min]*
(2/0)	98	2	—	1950	25
(5/1)	94	5	1	1920	20
(7/2)	91	7	2	1900	15
(10/1)	89	10	1	1900	—

[a] Including 2·72 wt% silica calculated from the O-content.

Typical time-dependent process conditions for a two-step sinter-HIP-process of silicon nitride are schematically shown in Fig. 1. The corresponding linear shrinkage was measured by a HIP-dilatometer and the densification rate was calculated. The shrinkage of the investigated samples with 2 wt% Y_2O_3 (2/0), 5 wt% Y_2O_3 / 1 wt% SiO_2 (5/1), and 7 wt% Y_2O_3 / 2 wt% SiO_2 (7/2) is characterised by three maxima. The first one corresponds to shrinkage by particle rearrangement, the second one by dissolution of α-Si_3N_4 and precipitation of β-Si_3N_4 and the third one is attributed to the dissolution of the transient formed crystalline secondary phase $Y_2Si_2O_7$ as determined by X-ray diffraction analysis. Dilatometric studies showed that pore closure could only be achieved after the onset of the third maximum. For the optimisation of the sintering programme, samples were heated up until the third maximum appears. The heating phase is followed by an isothermal sintering before the pressure is increased. The sintering temperature necessary to achieve the third maximum and the isothermal sintering time for the investigated compositions are given in Table 1. The isothermal sintering time has to be as short as possible in order to avoid grain growth since it would reduce further densification in the pressure stage.

A systematic variation of the compositions in the system Si_3N_4-Y_2O_3-SiO_2 in combination with a detailed analysis of their sintering behaviour exhibits the potential of the sinter-HIP-process. Fig. 2 shows a section of the phase diagram of the Si_3N_4–Y_2O_3-SiO_2 system[7] with the two tie-lines between Si_3N_4 and $Y_2Si_2O_7$ and Si_3N_4 and $Y_5(SiO_4)_3N$. The lowest possible "additive" content is given by the oxygen content of the Si_3N_4-powder. Complete densification (>98% th.d.) could only be obtained for compositions near the tie-line Si_3N_4–$Y_2Si_2O_7$.[11] The sample (2/0) with only 2 wt% Y_2O_3 and no additional silica has the lowest additive content. The composition is comparable to typical high-temperature resistant HIP-Si_3N_4 ceramics which are densified by glass encapsulation technique.[12,13] Samples out of the compositional range marked in Fig. 2 do not reveal pore closure during the first sintering step. The poor sinterability is due to the formation of Si_2N_2O (O-rich) or $Y_5(SiO_4)_3N$ (O-poor) and depends strongly on the Y_2O_3/SiO_2-ratio, but it is relatively independent of the total volume fraction of additives. Even materials with 10 wt% Y_2O_3, but only 1 wt% SiO_2 could not be densified by sinter-HIPing. The difference between a sinterable and non-sinterable material is demonstrated in Fig. 3. The development of the open and closed porosity as a function of the total porosity shows for sample (10/1) with 10 wt% Y_2O_3, and 1 wt% additional SiO_2 that the sintering ends at a total porosity of 12%. Most of the pores (10%) are open and no further densification could be expected by a pressure increase [Fig. 3(a)]. Specimen (2/0) shows a cross over of the lines for open and closed porosity. Pore closure is achieved at a total porosity of 8% so that the residual pores can be further eliminated by an external pressure [Fig. 3(b)].

The final density depends also on the applied HIP-pressure which was varied between 10 and 100 MPa in the second sintering step (Fig. 4). No pressure influence could be detected with respect to the size and morphology of the silicon nitride grains and the grain boundary phase. The density for the sample (2/0) with the lowest additive content increases with an increasing pressure, whereas the maximum density for the two additive-rich compositions (7/2) and (5/1) is already achieved at 50 MPa. A further pressure increase leads to a slight reduction of the density which is accompanied by the formation of large-scale inhomogeneities in near surface regions. These inhomogeneities can be explained by micropores formed during the pressure increase. When the

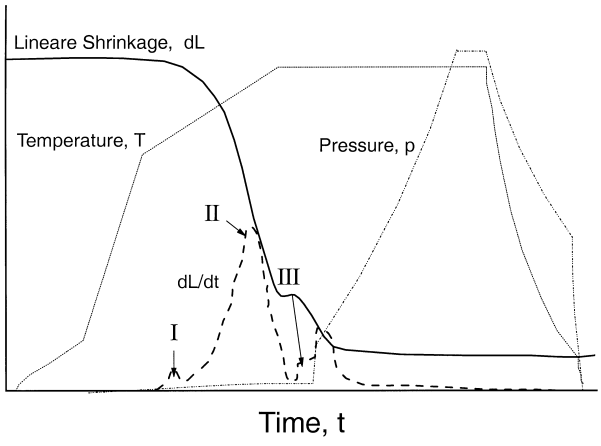

Fig. 1. Typical temperature and pressure programme for a two-step sinter-HIP-cycle with the corresponding linear shrinkage (dL) and shrinkage rate (dL/dt). Pore closure could only be obtained after the onset of the third shrinkage maximum.

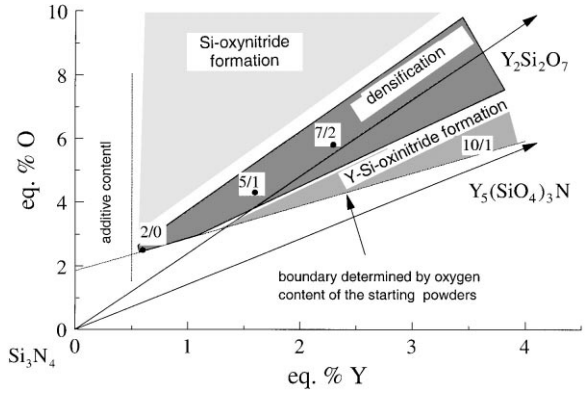

Fig. 2. Si_3N_4-rich corner of the Si_3N_4–SiO_2–Y_2O_3 subsolidus phase diagram with the compositional range for sinterable Y-based sinter-HIP materials.[11]

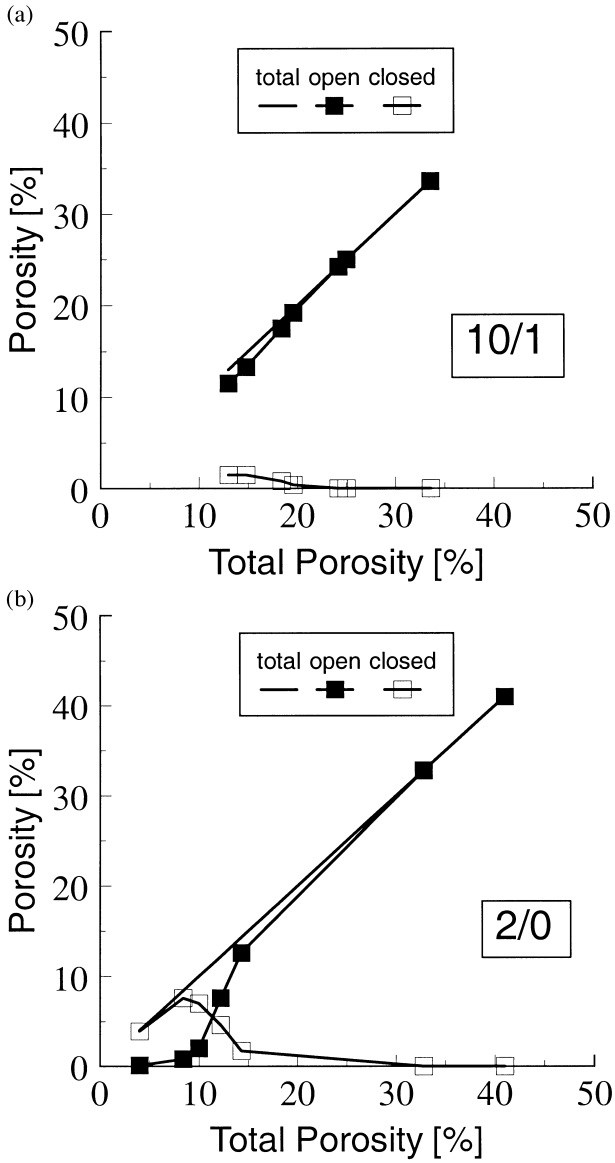

Fig. 3. Development of the open and closed porosity as a function of the total porosity in the low pressure sintering step for the compositions (a) 10/1 and (b) 2/0.

HIP-pressure exceeds a certain value (> 50 MPa for the compositions 5/1 and 7/2) the gas could penetrate through the grain boundary and some residual pores were filled with gas. Although these pores can be closed again in the isothermal HIP-step, a complete elimination is impossible due to the high internal pressure. Since microporosity could not be detected in sample (2/0), it is assumed that the micropore formation depends on the volume fraction of the additives as well as on the viscosity of the liquid phase.

3.2 Microstructural characterisation

Figure 5 shows the microstructure of the three investigated compositions. The samples (2/0) and (7/2) had a relatively homogeneous microstructure, while sample (5/1) shows a more bimodal grain size distribution with regions of smaller equiaxed grains. All compositions reveal elongated grains, but

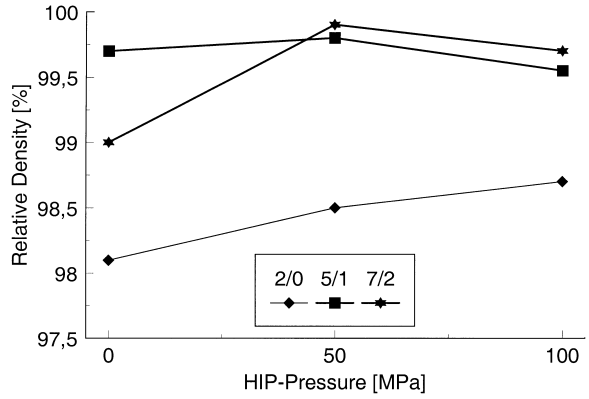

Fig. 4. Relative density as a function of the HIP-pressure. The maximum density for the additive-rich compositions 7/2 and 5/1 is already achieved at 50 MPa.

the mean grain size increases with higher additive contents. The microstructural development is normally controlled by the number of β-seeds in the Si_3N_4 starting powder and the volume fraction of the liquid phase.[14] The initial β-seeds are nearly the same for all compositions, but the volume fraction of the liquid phase increases with an increasing additive content. The increasing volume fraction of liquid phase has two effects: (i) the amount of Si_3N_4 powder which is dissolved during densification increases and leads to a faster phase transformation. Kinetic investigations reveal furthermore a shift in the temperature for the onset of phase transformation from 1550°C for composition (7/2) to 1720°C for (2/0). The different solubility of Si_3N_4 also has an influence on the number of growing β-seeds. This means that the critical seed size will increase with increasing amounts of the liquid phase[14]; (ii) a higher volume fraction of liquid phase reduces the grain impingement so that more crystals with a high aspect ratio will be formed.[15]

An analysis of the aspect ratio development for compositions (7/2) and (2/0) shows that the maximum mean aspect ratio can be obtained at the end of the phase transformation when the samples achieved approximately 90% relative density. The mean aspect ratio of the elongated grains, determined by the grain disintegration technique,[16] was 6.9 for sample (7/2) and 4·5 for sample (2/0). It decreases during further densification by solution precipitation of smaller β-grains to 3·9 for sample (7/2) and 3·8 for (2/0). The observations are in a good agreement with results reported earlier by Krämer *et al.*[17] They investigated the grain growth of silicon nitride in supersaturated oxynitride glasses and found that the reduction of the mean aspect ratio during Ostwald-ripening can be mainly attributed to the dissolution of grains with a small diameter, but high aspect ratios.

The compositions revealed an amorphous grain boundary phase after sinter-HIPing. However, the

secondary grain boundary phase γ-$Y_2Si_2O_7$ starts to crystallise during a thermal treatment in air at 1400°C for 200 h. Different HIP-pressures had no detectable influence on the grain boundary composition.

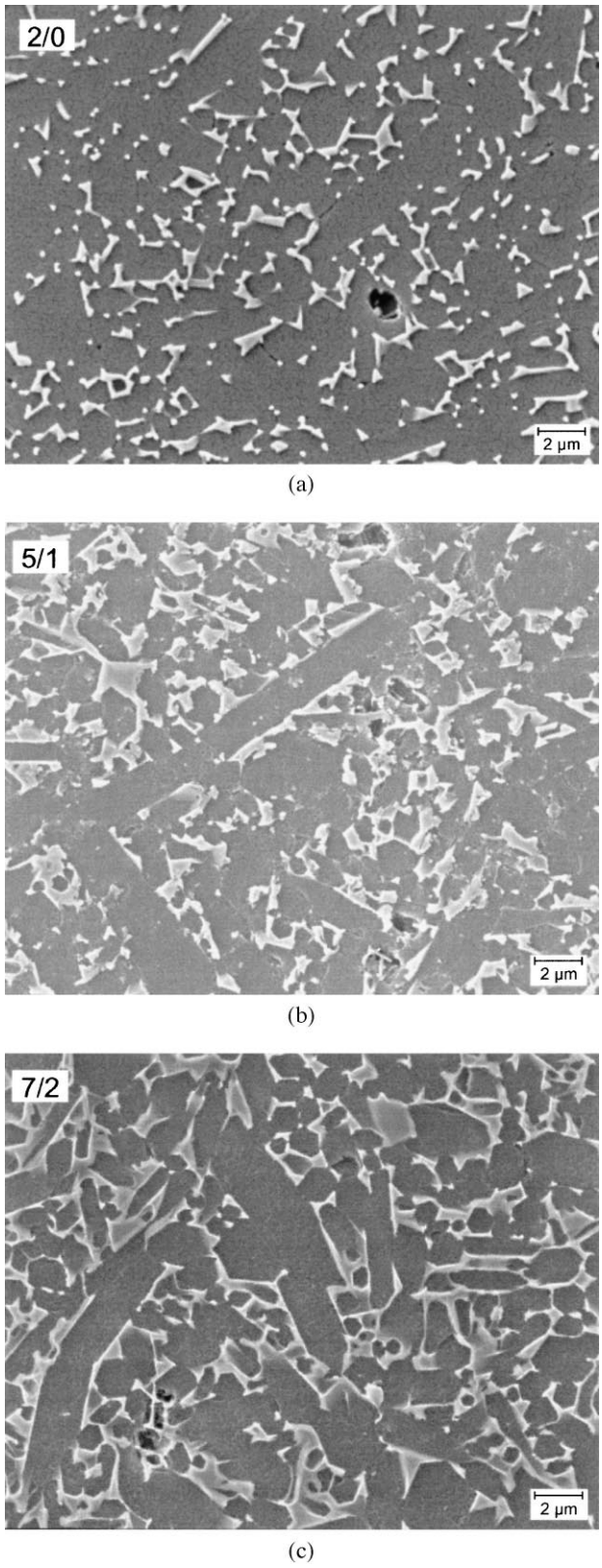

Fig. 5. SEM-micrographs of polished and plasma-etched surfaces of the samples (a) 7/2, (b) 5/1, and (c) 2/0. All samples reveal elongated grains; grain sizes increase with increasing additive content.

3.3 Mechanical properties

3.3.1 Bending strength and fracture toughness

The 4-point bending strength was measured at room temperature and 1400°C in order to study the influence of different processing parameters. The room temperature strength as a function of the HIP-pressure is shown in Fig. 6. The compositions (5/1) and (7/2) exhibit a maximum strength 873 and 841 MPa, respectively. Sample (2/0) has a maximum strength of only 461 MPa (Table 2). It is obvious that the strength increases significantly with increasing HIP-pressure despite the formation of microporosity in the near surface regions of the additive-rich samples. The strength increase with increasing HIP-pressure is attributed to a reduction of the critical flaw size. The difference in strength between the additive-rich compositions and sample (2/0) correlates with the fracture toughness: the as-sintered samples (7/2) and (5/1) had a toughness of 6·6 and 5·4 $MPam^{1/2}$, respectively, but sample (2/0) showed only 2·2 $MPam^{1/2}$. The significant lower fracture toughness for the (2/0) sample is related to a transition from an intergranular fracture mode to a mainly transgranular fracture mode as indicated in Fig. 7(a). The pre-oxidation leads to a small toughness increase of 0.3 $MPam^{1/2}$ for material (2/0), whereas the toughness of (5/1) and (7/2) decreases by 0·6 and 0·8 $MPam^{1/2}$, respectively (Table 3). The toughness decrease for the additive-rich compositions is attributed to the crystallization of the grain boundary phase.[4]

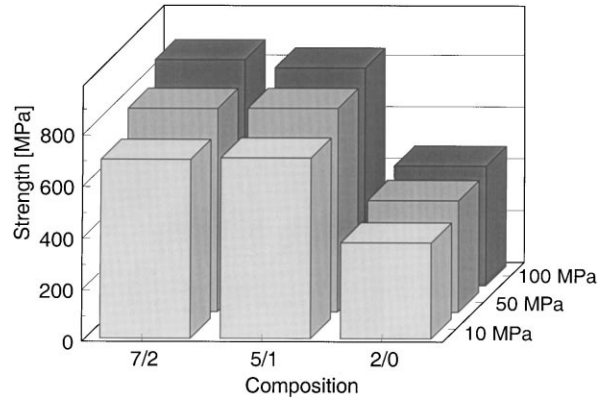

Fig. 6. Bending strength at room temperature as a function of HIP-pressure. All compositions reval the highest strength at the maximum pressure of 100 MPa.

Table 2. Influence of the HIP-pressure on the strength of as-sintered (a.s.) and pre-oxidised (ox.) samples

Bending strength [MPa]						
Pressure [MPa]	*(7/2)*		*(5/1)*		*(2/0)*	
	a.s.	*ox.*	*a.s.*	*ox.*	*a.s.*	*ox.*
10	693	510	699	550	373	414
50	787	612	788	661	433	604
100	873	647	841	669	461	531

Becher *et al.*[18] demonstrated that a high toughness (> 10 $MPa^{1/2}$) could be achieved by a bimodal grain size distribution with a high volume fraction of elongated grains in combination with a weak interface between the silicon nitride grains. Although, the interfacial strength is not known for the present materials, it is assumed that composition (2/0) exhibits a very strong interface. Therefore, it is concluded that even a higher volume fraction of elongated grains and an increase of the mean aspect ratio would not enhance toughness.

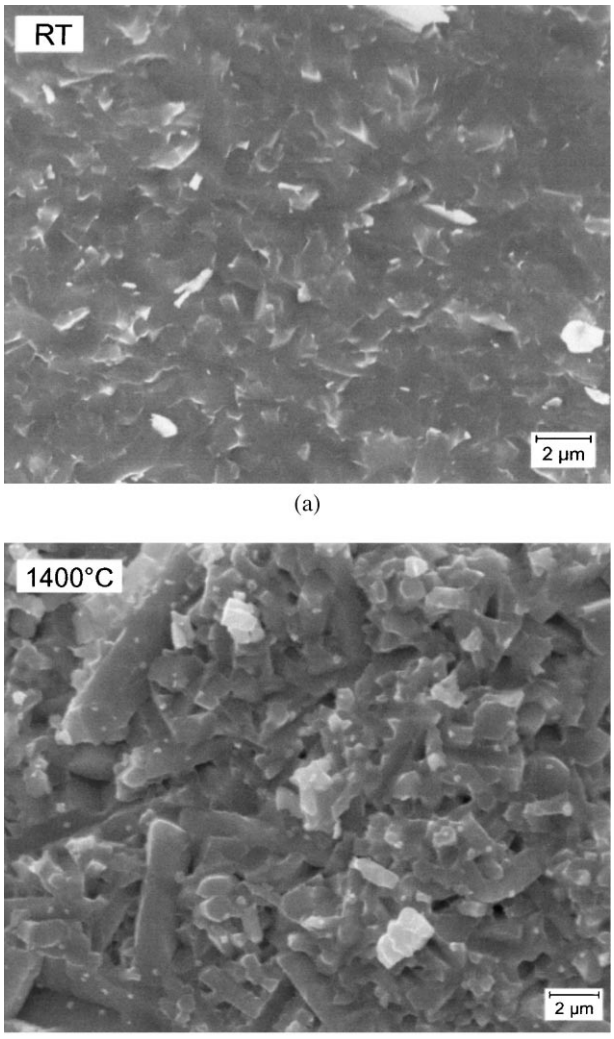

Fig. 7. SEM-micrographs of a fracture surface of material 2/0 after a test at (a) room temperature and (b) 1400°C indicate a transition from a transgranular to an intergranular fracture behaviour.

Table 3. Fracture toughness of as-sintered (a.s.) and pre-oxidised (ox.) samples

Fracture toughness [MPa·m$^{1/2}$]		
Sample	*a.s.*	*ox.*
(2/0)	2·2	2·5
(5/1)	5·4	4·8
(7/2)	6·6	5·8

Table 2 shows, additionally, the influence of an oxidation treatment for 200 h at 1400°C. The tests were performed directly after the oxidation treatment without further surface treatment. The additive-rich compositions (7/2) and (5/1) revealed a strength decrease of approximately 200 MPa due to surface damage during oxidation or the crystallisation of the grain boundary phase which could cause the formation of internal stresses.[19] Sample (2/0) shows the opposite effect: the strength is increased by 70 MPa, although grain boundary crystallisation occurs. The improvement could be related to a healing of cracks formed during machining of the relatively brittle material. Because of the high oxidation resistance, no damage of the near surface regions is expected during the thermal treatment.

Figure 8 shows the high-temperature strength at 1400°C after sinter-HIPing with a maxmimum pressure of 50 MPa and after pre-oxidation for 200 h at 1400°C. The additive-rich compositions (7/2) and (5/1) had a mean strength between 542 and 508 MPa. The similar strength for the as-sintered and heat-treated specimens supports the argument that the strength degradation at room temperature is mainly attributed to a grain boundary crystallisation which occurs during the measurement. A damage by oxidation could be neglected during the testing time. The pre-oxidised samples (2/0) as well as the as-sintered samples densified with 100 MPa pressure showed a strength increase from room temperature to 1400°C. Measurements of the pre-oxidised material up to a temperature of 1475°C indicate that the strength starts to decrease above 1400°C. However, the mean strength at 1475°C is still 478 MPa. Investigations of the fracture surface exhibit a change in the fracture mode from predominantly transgranular [Fig. 7(a)] to intergranular [Fig. 7(b)] — 1400°C. The effect could be explained by a weakening of the grain boundary phase. Therefore, it can be assumed that the strength increase from room temperature to

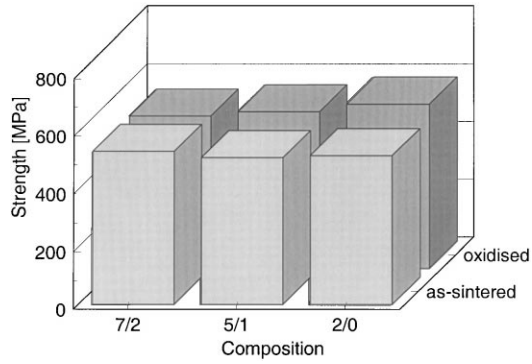

Fig. 8. Bending strength at 1400°C for as-sintered and pre-oxidised samples indicate a strength improvement by the thermal treatment for 200 h at 1400°C.

1400°C is attributed to a simultaneous increase in fracture toughness.

3.3.2 Creep behaviour

The creep resistance of dense silicon nitride ceramics is controlled by the size and morphology of the Si_3N_4 grains as well as the chemical composition of the grain boundary phase which is determined by the additive system and the silica content of the silicon nitride powder. For the discussion of the grain boundary region, it is nescessary to distinguish between triple junctions and grain boundary films between two adjacent Si_3N_4 grains. The triple junctions could be crystallise during thermal treatment, while grain boundary films are in general amorphous. The film thickness depends on the additive system and varies between 0·1 and 0·2 nm, but it is constant for a given composition.[20]

All measurements were performed with pre-oxidised samples in order to avoid any microstructural change during the creep test. This means that the triple junctions consist of the crystalline secondary phase $Y_2Si_2O_7$. Figure 9(a) exhibits the creep strain as a function of time. Both additive-rich compositions reveal a similar creep deformation of 0·27% after 100 h. The transition from primary to stationary creep is not well defined. Specimen (2/0) exhibits a total creep strain of 0·08% after 100 h, but most of the deformation (0·6%) happens during the first 2 h within the primary creep regime. The minimum creep rates for the temperature range between 1300 and 1450°C are given in Fig. 9(b). The composition with lowest additive content shows the lowest creep rate of the investigated samples with values of $1{\cdot}5\times10^{-9}$ s^{-1} at 1400°C and an activation energy of 157 kJ/mol. The materials (7/2) and (5/1) had a creep rate of 7×10^{-9} s^{-1} at 1400°C and an activation energy of approximately 350 kJ/mol. Experimental data from bending creep tests are not accurate enough to study the creep mechanism. Nevertheless, it is possible to discuss the difference between the tested materials. From the nearly identical creep behaviour of the additive-rich samples it can be concluded that a higher additive content does not necessarily decrease the creep resistance as long as the triple junctions are crystallised.[19] Since primary creep is mainly attributed to grain boundary sliding,[21] both materials must have a similar composition of the grain boundary films. The local grain boundary chemistry for material (2/0) has to be different since this composition exhibits a better creep resistance and also a lower room temperature fracture toughness which is evidence for a strong interfacial bonding between the silicon nitride grains. A comparison of the present material (2/0) with a glass-encapsulated

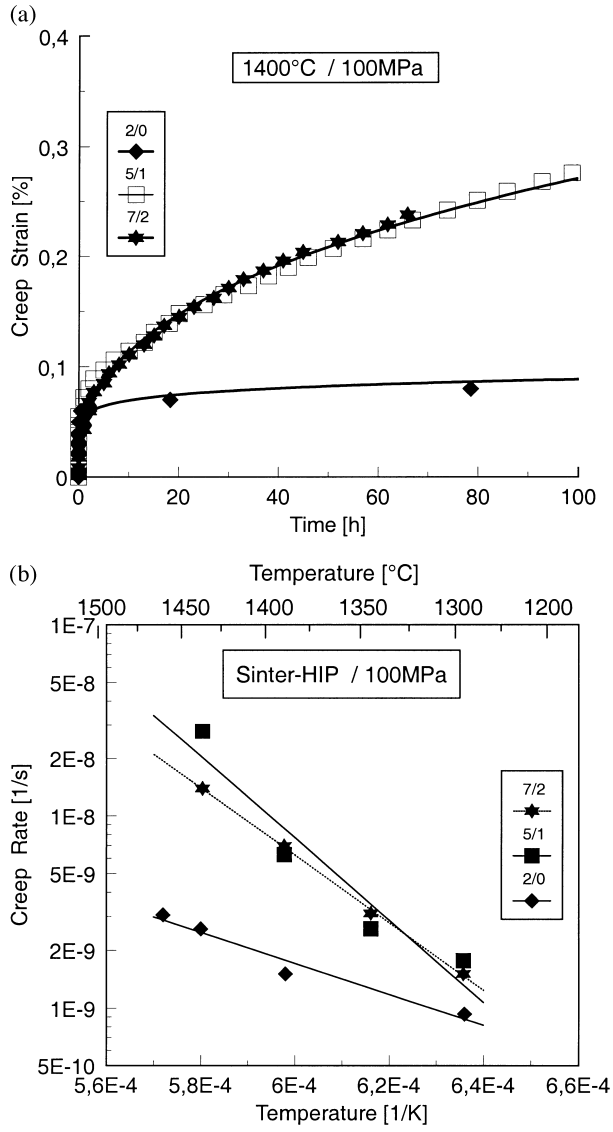

Fig. 9. Creep behaviour at 1400°C of the additive-rich compositions 7/2 and 5/1 in comparison to composition 2/0. (a) creep deformation at 100 MPa and (b) temperature dependency of the minimum creep rates.

HIP-Si_3N_4 prepared by Tanaka,[22] which contains only silica from the surface of the Si_3N_4 powder, shows similar properties for the two ceramics. The present material has a slightly higher strength and creep resistance, but both exhibit an extremely low fracture toughness between 2·5 and 3 $MPam^{1/2}$. Since high toughness and high strength require a weak interfacial bonding it seems to be not possible to achieve simultaneously excellent high temperature properties.

4 Conclusions

The additive content of dense Y_2O_3/SiO_2 containing silicon nitride ceramics could be reduced to 2 wt% Y_2O_3 by a two-step sinter-HIP-process with maximum pressures of 100 MPa. However, complete densification is restricted to compositions

near the tie-line between Si_3N_4 and $Y_2Si_2O_7$. For materials with higher or lower Y_2O_3/SiO_2-ratios, the liquid phase starts to crystallise during densification and pore closure could not be obtained during the low pressure sintering stage. Systematic studies of the influence of the additive content on the mechanical properties showed that an additive reduction is combined with a significant decrease in fracture toughness. The increase in brittleness is attributed to a strong interface between the silicon nitride grains and correlates with a transition from an intergranular to a mainly transgranular fracture mode. Nevertheless, the material with the lowest additive content (2 wt% Y_2O_3) exhibits no strength degradation up to 1400°C and relatively small creep rates ($1{\cdot}5\times10^{-9}$ s^{-1} at 1400°C/100 MPa) in contrast to the additive-rich compositions with 5 and 7 wt% Y_2O_3, respectively.

References

1. Tani, E., Umebayashi, Kishi K. and Kobayashi, K., Gas-pressure sintering of Si_3N_4 with concurrent addition of Al_2O_3 and 5 wt% rare earth oxide: high fracture toughness Si_3N_4 with fiber-like structure. *Am. Ceram. Soc. Bull.*, 1986, **65**(9), 1311.
2. Mitomo, M., Hirosaki, N. and Hirotsuru, H., Microstructural design and control of silicon nitride ceramics. *MRS Bulletin*, 1995, **XX**(2), 38.
3. Becher, P. F., Microstructural design of toughened ceramics. *J Am. Ceram. Soc.*, 1991, **74**, 255.
4. Hoffmann, M. J., High-temperature properties of Si_3N_4 ceramics. *MRS Bulletin*, 1995, **XX** (2), 28.
5. Lewis, M. H., Sialons and silicon nitrides; microstructural design and performance. In *Silicon Nitride Ceramics — Scientific and Technological Advances*, ed. I. -W. Chen, P. F. Becher, M. Mitomo, G. Petzow and T.-S. Yen, MRS Symposium Proceedings, Vol. 287, MRS, Pittsburgh, PA, 1993, p. 159.
6. Yen, T.-S. and Sun, W. Y., Phase relationship studies of silicon nitride system — a key to materials design. In *Silicon Nitride Ceramics — Scientific and Technological Advances*, ed. I. -W. Chen, P. F. Becher, M. Mitomo, G. Petzow and T.-S. Yen, MRS Symposium Proceedings, Vol. 287, MRS, Pittsburgh, PA, (1993), 39.
7. Gaukler, L. J., Hohnke, H. and Tien, T. Y., The system Si_3N_4-SiO_2-Y_2O_3. *J. Am. Ceram. Soc.*, 1980, **63**(1–2), 35.
8. Kühne, A., Oberacker, R. and Thümmler, F., HIP-dilatometer for process development in powder materials. *Powder Metallurgy In.*, 1991, **23**(2), 113.
9. Täffner, U., Hoffmann, M. J., Krämer, M. and Petzow, G., A comparison between different etching methods for silicon nitride ceramics. *Practical Metallography*, 1990, **27**, 385.
10. Warren, R. and Johannesson, B., Creation of stable cracks in hard metals using "bridge" indentation. *Powder Metallurgy*, 1984, **27**, 25–29.
11. Geyer, A., Potential of the sinter-HIP-process for the development of silicon nitride materials for high-temperature applications. Dissertation, University of Karlsruhe, 1998.
12. Sanders, W. A. and Groseclose, L. E., Flexural stress rupture and creep of selected commercial silicon nitrides. *J. Am. Ceram. Soc.*, 1993, **76**(2), 553.
13. Wiederhorn, S. M., Hockey, B. J. and Cranmer, D. C., Transient creep behaviour of hot isostatically pressed silicon nitride nitride. *J. Mater. Sci.*, 1993, **28**, 445.
14. Hoffmann, M. J. and Petzow, G., Tailored microstructures of silicon nitride ceramics. *Pure and Appl. Chem.*, 1994, **66**(9), 1807.
15. Dressler, W., Kleebe, H.-J., Hoffmann, M. J., Rühle, M. and Petzow, G., Model experiments concerning abnormal grain growth in silicon nitride. *J. Eur. Ceram. Soc.*, 1996, **16**, 3.
16. Geyer, A. and Oberacker, R., Quantitative characterisation of microstructural development in silicon nitride by a grain disintegartion technique. *MC 95 International Metallography Conference*, ASM International, 1996, p. 205.
17. Krämer, M., Hoffmann, M. J. and Petzow, G., Growth kinetics of Si_3N_4 during α/β-transformation. *Acta Metall. mater.*, 1993, **41**(10), 2939.
18. Becher, P. F., Sun, E. Y., Plucknett, K. P., Alexander, K. B., Hsueh, C.-H., Lin, H. T., Waters, S. B., Westmoreland, C. G., Kang, E.-S., Hirao, K., Brito, M. E., Microstructural design of silicon nitride with improved fracture toughness, part I: Effects of grain shape and size. *J. Am. Ceram. Soc.*, in press.
19. Hoffman, M. J., High-temperature properties of Yb-containing Si_3N_4. In: *Tailoring of Mechanical Properties of Si_3N_4 Ceramics*, ed. M. J. Hoffman and G. Petzow, NATO ASI, Series E, Kluwer Academic Press, Dordrecht, 1994, pp. 233.
20. Kleebe, H.-J., Cinibulk, M. K., Cannon, R. M. and Rühle, M., Statistical analysis of the intergranular film thickness in silicon nitride ceramics. *J. Am. Ceram. Soc.*, 1993, **76**(9), 1969.
21. Wilkinson, D. S., Creep mechanics in silicon nitride ceramics. In: *Tailoring of Mechanical Properties of Si_3N_4 Ceramics*, ed. M. J. Hoffman and G. Petzow, NATO ASI, Series E, Kluwer Academic Press, Dordrecht, 1994, pp. 233.
22. Tanaka, I., Pezotti, G., Okamoto, T., Miyamoto, Y. and Koizumi, M., Hot isostatic press sintering and properties of silicon nitride without additives. *J. Am. Ceram. Soc.*, 1989, **72**(9), 1656.